



Fabrication of tunable chirped mPOF Bragg gratings using a uniform phase mask

RUI MIN,^{1,*} BEATRIZ ORTEGA,¹ AND CARLOS MARQUES²

¹ITEAM Research Institute, Universitat Politècnica de València, Valencia, Spain

²Instituto de Telecomunicações and Physics Department & I3N, Universidade de Aveiro, Portugal

*rumi@doctor.upv.es

Abstract: We demonstrate chirped Bragg gratings fabrication in doped microstructured tapered polymer fibers by using a uniform phase mask. The use of high photosensitive benzyl dimethyl ketal (BDK) doped core fiber allows to obtain chirped Bragg gratings by means of a single krypton fluoride laser pulse. The stability of the gratings has been confirmed and the strain and temperature sensitivity measurements demonstrate their tunable properties. Finally, different tapered profiles have been implemented in order to show the potentiality of this fabrication technique in polymer optical fibers.

© 2018 Optical Society of America under the terms of the [OSA Open Access Publishing Agreement](#)

OCIS codes: (060.3738) Fiber Bragg gratings, photosensitivity; (130.5460) Polymer waveguides.

References and links

1. K. O. Hill, F. Bilodeau, B. Malo, T. Kitagawa, S. Thériault, D. C. Johnson, J. Albert, and K. Takiguchi, "Chirped in-fiber Bragg gratings for compensation of optical-fiber dispersion," *Opt. Lett.* **19**(17), 1314–1316 (1994).
2. B. Ortega, J. L. Cruz, J. Capmany, M. V. Andres, and D. Pastor, "Variable delay line for phased-array antenna based on a chirped fiber grating," *IEEE Trans. Micro. Theory* **48**(8), 1352–1360 (2000).
3. C. Wang and J. Yao, "A nonuniformly spaced microwave photonic filter using a spatially discrete chirped FBG," *IEEE Photonics Technol. Lett.* **25**(19), 1889–1892 (2013).
4. O. Frazão, M. Melo, P. V. S. Marques, and J. L. Santos, "Chirped Bragg grating fabricated in fused fibre taper for strain-temperature discrimination," *Meas. Sci. Technol.* **16**(4), 984–988 (2005).
5. H. Chang, Y. Chang, H.-J. Sheng, M.-Y. Fu, W.-F. Liu, and R. Kashyap, "An ultra-sensitive liquid-level indicator based on an etched chirped-fiber Bragg grating," *IEEE Photonics Technol. Lett.* **28**(3), 268–271 (2016).
6. J. Lauzon, S. Thibault, J. Martin, and F. Ouellette, "Implementation and characterization of fiber Bragg gratings linearly chirped by a temperature gradient," *Opt. Lett.* **19**(23), 2027–2029 (1994).
7. P. C. Hill and B. J. Eggleton, "Strain gradient chirp of fibre Bragg gratings," *Electron. Lett.* **30**(14), 1172–1174 (1994).
8. R. Kashyap, P. F. McKee, R. J. Campbell, and D. L. Williams, "Novel method of producing all fibre photoinduced chirped gratings," *Electron. Lett.* **30**(12), 996–998 (1994).
9. J. L. Cruz, L. Dong, S. Barcelos, and L. Reekie, "Fiber Bragg gratings with various chirp profiles made in etched tapers," *Appl. Opt.* **35**(34), 6781–6787 (1996).
10. D. J. Webb, "Fibre Bragg grating sensors in polymer optical fibres," *Meas. Sci. Technol.* **26**(9), 092004 (2015).
11. C. A. F. Marques, D. J. Webb, and P. Andre, "Polymer optical fiber sensors in human life safety," *Opt. Fiber Technol.* **36**, 144–154 (2017).
12. I. Tafur Monroy, H. P. A. vd Boom, A. M. J. Koonen, G. D. Khoe, Y. Watanabe, Y. Koike, and T. Ishigure, "Data transmission over polymer optical fibers," *Opt. Fiber Technol.* **9**(3), 159–171 (2003).
13. A. Nespola, S. Abrate, R. Gaudino, C. Zerna, B. Offenbeck, and N. Weber, "High-Speed Communications Over Polymer Optical Fibers for In-Building Cabling and Home Networking," *IEEE Photonics J.* **2**(3), 347–358 (2010).
14. X. Hu, D. Saez-Rodriguez, C. Marques, O. Bang, D. J. Webb, P. Mégret, and C. Caucheteur, "Polarization effects in polymer FBGs: study and use for transverse force sensing," *Opt. Express* **23**(4), 4581–4590 (2015).
15. X. Hu, C. F. Pun, H. Y. Tam, P. Mégret, and C. Caucheteur, "Tilted Bragg gratings in step-index polymer optical fiber," *Opt. Lett.* **39**(24), 6835–6838 (2014).
16. L. P. Pereira, A. Pospori, M. F. Domingues, P. Antunes, S. Marques, O. Bang, D. J. Webb, and C. Marques, "Phase-shifted Bragg grating inscription in PMMA microstructured POF using 248 nm UV radiation," *J. Lightwave Technol.* **99**, in press (2017).
17. H. Liu, H. Liu, G. Ding Peng, and T. W. Whitbread, "Tunable dispersion using linearly chirped polymer optical fiber Bragg gratings with fixed center wavelength," *IEEE Photonics Technol. Lett.* **17**(2), 411–413 (2005).
18. C. A. F. Marques, P. Antunes, P. Mergo, D. J. Webb, and P. André, "Chirped Bragg gratings in PMMA step-index polymer optical fiber," *IEEE Photonics Technol. Lett.* **29**(6), 500–503 (2017).

19. D. Sáez-Rodríguez, K. Nielsen, H. K. Rasmussen, O. Bang, and D. J. Webb, "Highly photosensitive polymethyl methacrylate microstructured polymer optical fiber with doped core," *Opt. Lett.* **38**(19), 3769–3772 (2013).
20. X. Hu, G. Woyessa, D. Kinet, J. Janting, K. Nielsen, O. Bang, and C. Caucheteur, "BDK-doped core microstructured PMMA optical fiber for effective Bragg grating photo-inscription," *Opt. Lett.* **42**(11), 2209–2212 (2017).
21. A. Pospori, C. A. F. Marques, O. Bang, D. J. Webb, and P. André, "Polymer optical fiber Bragg grating inscription with a single UV laser pulse," *Opt. Express* **25**(8), 9028–9038 (2017).
22. C. A. F. Marques, A. Pospori, G. Demirci, O. Çetinkaya, B. Gawdzik, P. Antunes, O. Bang, P. Mergo, P. André, and D. J. Webb, "Fast Bragg grating inscription in PMMA polymer optical fibres: impact of thermal pre-treatment of preforms," *Sensors (Basel)* **17**(4), 891 (2017).
23. D. Sáez-Rodríguez, R. Min, B. Ortega, K. Nielsen, and D. J. Webb, "Passive and Portable Polymer Optical Fiber Cleaver," *IEEE Photonics Technol. Lett.* **28**(24), 2834–2837 (2016).
24. K. Bhowmik, G.-D. Peng, Y. Luo, E. Ambikairajah, V. Lovric, W. R. Walsh, and G. Rajan, "Etching process related changes and effects on solid-core single-mode polymer optical fiber grating," *IEEE Photonics J.* **8**(1), 1–9 (2016).
25. K. Bhowmik, G.-D. Peng, E. Ambikairajah, V. Lovric, W. R. Walsh, B. G. Prusty, and G. Rajan, "Intrinsic high-sensitivity sensors based on etched single-mode polymer optical fibers," *IEEE Photonics Technol. Lett.* **27**(6), 604–607 (2015).
26. C. A. F. Marques, *Fiber-Optic Components for Optical Communications and Sensing*, PhD Thesis, University of Aveiro, (2013).
27. L. Dong, J. L. Cruz, L. Reekie, and J. A. Tucknott, "Fabrication of chirped fibre gratings using etched tapers," *Electron. Lett.* **31**(11), 908–909 (1995).
28. M. A. Putnam, G. M. Williams, and E. J. Friebele, "Fabrication of tapered, strain-gradient chirped fibre Bragg gratings," *Electron. Lett.* **31**(4), 309–310 (1995).

1. Introduction

Chirped Bragg gratings are promising devices in optical fiber technology due to their well-known applications such as dispersion compensation [1], beam forming [2], microwave photonics filtering [3] and a variety of sensing applications [4, 5]. Several different chirping methodologies have been demonstrated in silica fiber. Previous works demonstrate chirped gratings fabrication by using refractive index gradient [1], temperature gradient [6], strain gradient [7] and also, varying the period of the grating [8]. Actually, the use of chirped phase mask is the most convenient way to fabricate chirped Bragg gratings by a single exposure process. This method offers high repeatability and easy implementation. However, fabricated gratings are limited by the phase mask chirp and a number of phase masks are required to fabricate gratings with different chirp parameters, which leads to an expensive technique. Oppositely, chirped Bragg gratings irradiated under strain gradient offer flexibility since the fiber is subjected under strain which is modified during the UV beam scanning and therefore, the chirp parameter can be accurately controlled [7]. Furthermore, non-uniform fiber diameter is obtained by tapering the fiber and applied strain results in a strain gradient. Consequently, different chirp parameters can be obtained by accurately control of the etching process [9].

Polymer optical fibers (POFs) have some advantages compared to silica fibers, such as a lower Young's modulus, a higher thermo-optic coefficient and a larger elongation before breakage which are exploited in a large variety of applications in sensing and telecommunications field [10–13]. Fabrication of polymer optical fiber Bragg gratings (POFBGs) is under research during the last two decades where recent achievements include uniform fiber Bragg gratings (FBGs) [10], birefringent Bragg gratings [14], tilted fiber Bragg gratings [15] and phase-shifted grating [16]. Unlike chirped Bragg gratings fabrication in silica fiber is a mature technology, chirped gratings in POFs are still a challenge. In 2005, a simple method based on axial tension and uniform heating was theoretically proposed to obtain linearly chirped Bragg gratings in POF tapers [17]. However, the first chirped POFBG was successfully fabricated by using a chirped phase mask in 2017 [18]. Nevertheless, this latter result was obtained by using special phase masks, leading to expensive and fixed fabrication parameters. Flexible fabrication techniques based on uniform phase masks are then required to be adopted as mass production of these optical components for different applications.

Regarding the UV-induced refractive index change in POF, high photosensitivity benzyl dimethyl ketal (BDK) doped microstructured POFs (mPOFs) have been recently reported [19,20]. The use of 248 nm UV pulsed laser system has been proposed to obtain the shortest time Bragg gratings fabrication with a single pulse Bragg gratings fabrication in doped fibers [21] and with few pulses using undoped fibers [22].

To the best of our knowledge, in this paper we present the first chirped Bragg grating in POF fabricated by using a uniform phase mask. Tapered optical fibers in the grating segment are employed in combination with strain in order to obtain tunable chirped Bragg gratings in microstructured BDK core doped POF.

2. Basics of chirped Bragg grating using tapered fibers

Considering a grating written in a tapered fiber with radius profile $r(z)$ under external tension F along the fiber axis. The Bragg wavelength, λ_B , shifts $\Delta\lambda_B(z)$ at z position, which can be calculated as [9]:

$$\frac{\Delta\lambda_B(z)}{\lambda_B} = (1 - p_e) \frac{F}{\pi E r(z)^2} \quad (1)$$

where E is Young's modulus and $p_e = 0.04$ is the photoelastic constant for polymer material. As a result, the inscription of a Bragg grating using a phase mask with uniform period leads to a chirped grating with a chirp profile given by the radius profile of the taper and the tension applied to the fiber during fabrication. The Bragg wavelength along the grating is given by:

$$\lambda_B(z) = \lambda_B(0) + \lambda_B \cdot f(z) \quad (2)$$

where $\lambda_B(0)$ is the Bragg wavelength at $z = 0$ and $\Delta\lambda_B$ is the total chirp of the grating. The chirp function of the chirped gratings $f(z)$ and the fiber radius $r(z)$ are related by the following expression [9]:

$$r(z) = \frac{r(0)r(L)}{\sqrt{[r(0)^2 - r(L)^2]f(z/L) + r(L)^2}} \quad (3)$$

where L is the grating length. Therefore, by accurate control of $r(z)$, it is easy to obtain various chirped grating profiles when the external tension is applied.

3. Experimental chirped fiber Bragg gratings using etched technology

All fibers used in this work were pre-annealed at 70°C for 12 hours, to remove any residual stresses created during the drawing process and also to remove possible twists present on it. Each fiber sample (long POF pieces up to 20 cm) were cleaved using a portable cleaver [23] and attached to demountable FC/PC connectors in order to simplify the interrogation of the POFBG. The use of tapered POFs to fabricate Bragg gratings with high performance utilizing the material changes exhibited in the POF due to etching process was well demonstrated in [24]. Pure acetone can be efficiently used to remove the cladding of PMMA POF. Two different POFs were used: a) PMMA mPOF with a three-ring cladding microstructure and BDK doped core close to endlessly single-mode (Fiber 1) [19] and b) Endlessly single-mode PMMA mPOF with BDK produced using the selected center hole doping technique (Fiber 2) [20]. Fiber 1 shows an average hole diameter and pitch of 1.74 μm and 3.7 μm respectively, with the external and core diameter of 130 μm and 8 μm , respectively. The ratio of the hole diameter to the pitch was calculated to be 0.47, therefore, the fiber could have either a single or a few modes, depending on the wavelength. Fiber 2 has the average hole diameter and pitch of 1.5 μm and 3.79 μm , respectively. Thus, the ratio of the hole diameter to the pitch was calculated to be 0.4, confirming that the mPOF is endlessly single-mode [20]. The

diameters of the core and the cladding are $6\ \mu\text{m}$ and $150\ \mu\text{m}$, respectively. Each piece of fiber used in this work was tilted and immersed in a container full of acetone in order to get different radius along the fiber based on the volatile property of acetone (see Fig. 1(a)). The etching time depends on the required cladding thickness [25]. Figure 1(b) shows an example of linearly tapered fiber with $L = 1\ \text{cm}$, $r(0) = 64\ \mu\text{m}$ and $r(L) = 55\ \mu\text{m}$. Due to the limited of microscope sight, here we just show a part of L , instead of the total length.

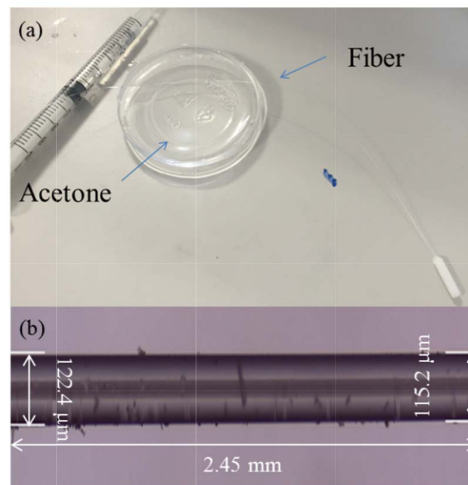


Fig. 1. (a) Photograph of acetone container, (b) Linearly tapered fiber profile showing a part of L .

A Coherent Bragg Star Industrial-LN krypton fluoride (KrF) excimer laser system operating at 248 nm wavelength was employed for the chirped Bragg grating inscription with a 2.5 mJ energy per pulse. The laser beam profile was measured as a rectangular Tophat function of $6.0 \times 1.5\ \text{mm}^2$ size and divergence $2 \times 1\ \text{mrad}^2$. The laser beam is focused in the fiber core utilizing a plano-convex cylindrical lens (Newport CSX200AR.10) with effective focal length of 200.0 mm. The effective spot size of the beam on the fiber surface is 16.0 mm in width and $32.4\ \mu\text{m}$ in height. For the grating inscription, we used the typical phase mask technique as depicted in Fig. 2. A 10 mm long uniform phase mask, which defines the physical length of the grating structure, of 567.8 nm period was employed in the setup and the grating is subjected to 1% strain during fabrication. The reflected optical power by the FBG was monitored during irradiation by employing a super luminescent diode (Superlum SLD-371-HP1) and an optical spectrum analyzer (Yokogawa AQ6373B) with 0.02 nm resolution bandwidth. A cross-section image of the Fiber 1 is shown in inset of Fig. 2.

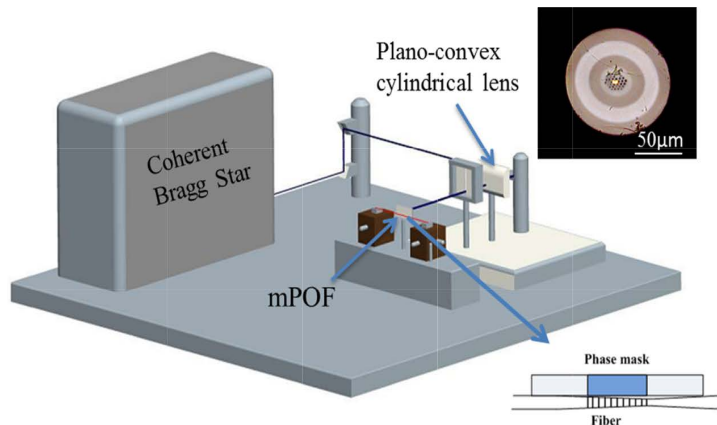


Fig. 2. (a) Experimental setup for chirped Bragg grating inscription based on uniform phase mask. Inset: mPOF cross-section (Fiber 1).

Figure 3 shows the 1 cm long grating response of Fiber 1 just after fabrication where a 0.26 nm chirp was created due to 1% strain applied to the 1 cm long linear taper where initial and final diameter are 128 μm and 110 μm , respectively, being ($r(0) = 64 \mu\text{m}$ and $r(L) = 55 \mu\text{m}$), which leads to a taper of 9 $\mu\text{m}/\text{cm}$. Figure 3 also shows a uniform Bragg grating with the sake of comparing it with the chirped grating obtained under 1.0% strain. We can observe that the uniform Bragg grating, fabricated on a not tapered optical fiber piece under 1% strain, reflects a narrower and stronger bandpass compared with the chirped one [26]. The higher bandwidth of the chirped grating is directly related with the linear variation of the period since the resonance condition occurs for various wavelengths, resulting in a grating with a bandwidth much higher than conventional FBGs.

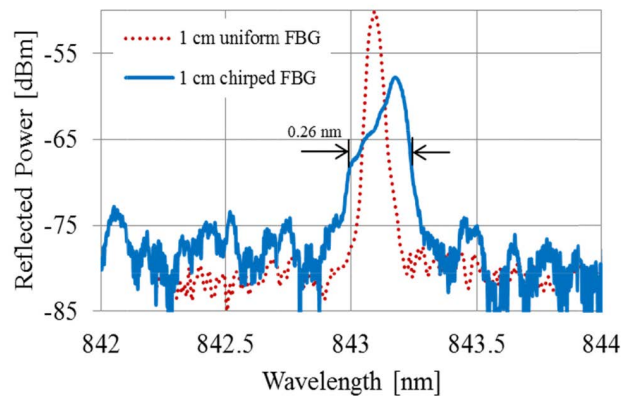


Fig. 3. Reflected optical power by the FBG fabricated on a 1% strained tapered fiber section obtaining a chirped FBG. Also, reflected spectrum of a uniform FBG for comparison with chirped grating after irradiation.

It shall be noted that the method used in this work is applying tension to the fiber during the inscription process. The grating is chirped during inscription due to the stress-optic effect caused by the strain gradient along the fiber. When the tension is removed, the chirp due to the stress-optic effect disappears, but another chirp is developed as different parts of the taper relax differently from the initial strain gradient. The same phenomenon occurs using tapered silica fibers [27]. Using this method presented here, the chirped grating can be packaged as

strain-free. It can create a larger chirp (than the method with no strain applied) for the same applied strain level, because the stress-optic effect has an opposite sign to the lengthening effect, and a chirp cancellation occurs.

Then, after two minutes of the fabrication we increase the strain to demonstrate the stability of the chirped grating. Figure 4 shows the spectrum of the reflected power when 1.3% strain was applied; the initial bandwidth was 0.7 nm (see red line in Fig. 4 (a)) but it increased up to 1.25 nm in 160 s (see blue line in Fig. 4(a)) due to the photosensitivity increase of BDK doped fiber, similar to post growth performance described in [21]. Figure 4(b) shows the chirped POFBG reflected bandwidth response evolution in time. From Fig. 4 we can notice a slight instability of the response over the time and it shall be noted that this results were collected after two minutes of the fabrication where the grating is in growing and spectral stabilization process [21]. The time to reach stability was around 280 s and the temporal stability in this case affects the bandwidth, but surprisingly not the reflected power [21]. So far it is still not clear about the mechanism. But we do believe that the thermal stress induced by UV irradiation in POF plays an important role. The thermal stress might induce the refractive index change with an opposite sign of that induced by UV photoreactions to the polymer fiber. The polymer FBG becomes stable when the thermal stress is completely relaxed. After this, the grating presents high level of stability for a long time (controlling the environmental room conditions).

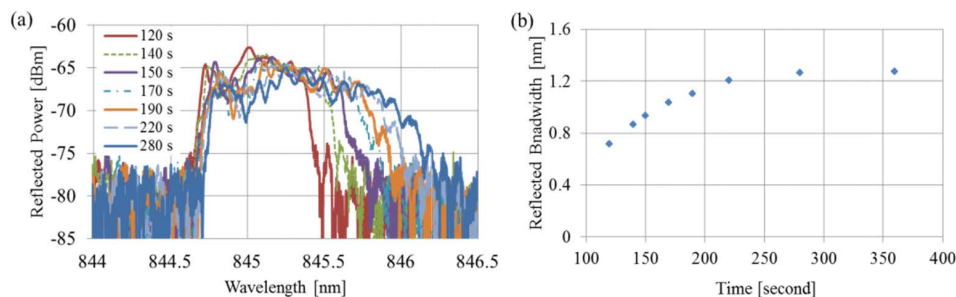


Fig. 4. (a) Reflected power by chirped POFBG (Fiber 1) under 1.3% strain two minutes after irradiation. (b) Chirped POFBG optical bandwidth response vs time during 360 seconds.

4. Strain and temperature response of chirped fiber Bragg grating

After the previous experiment, we released the strain and the resonance shifted to 835 nm with 1.6 nm bandwidth as displayed in Fig. 5(a). Similar performance happens in tapers fabrication using silica fibers where the strain gradient is formed along the grating when the fiber is held under tension producing a varying shift in the periodic refractive index and consequently, results in a tunable chirped grating [28]. As long as the strain is increased, the POFBG reflected spectral bandpass narrows up to 1% strain condition (irradiation was carried out under 1% strain) whereas additional strain causes a central wavelength shift to longer wavelengths as well as broader bandwidths, as shown in Fig. 5(a). Figures 5(b) and 5(c) show the spectral response of two gratings fabricated in two different tapered sections of Fiber 1 with $r(0) = 63 \mu\text{m}$ and $r(L) = 59 \mu\text{m}$ (taper of $4 \mu\text{m}/\text{cm}$) and $r(0) = 64 \mu\text{m}$ and $r(L) = 50 \mu\text{m}$ (taper of $14 \mu\text{m}/\text{cm}$), respectively, under different strain conditions. The grating in Fig. 5(b) shows a narrower bandwidth than the one depicted in Fig. 3. Only 0.5 nm bandwidth is observed after the strain release whereas 1 nm bandwidth is measured under 1.65% strain. However, the grating in Fig. 5(c) shows a 2.6 nm bandwidth under 1.50% strain which is broader than others due to the strong tapered profile also showing a high strain sensitivity [27]. It shall be noted that the deep peak in reflected bandwidth of chirped fiber Bragg grating under 1.50% strain (see Fig. 6(c)) is due to some mismatch in the position of the grating respect to the tapered section, which will become more clear with strain increase. An accurate

and smooth control of such strong tapered profiles is required by using expensive and high resolution setup.

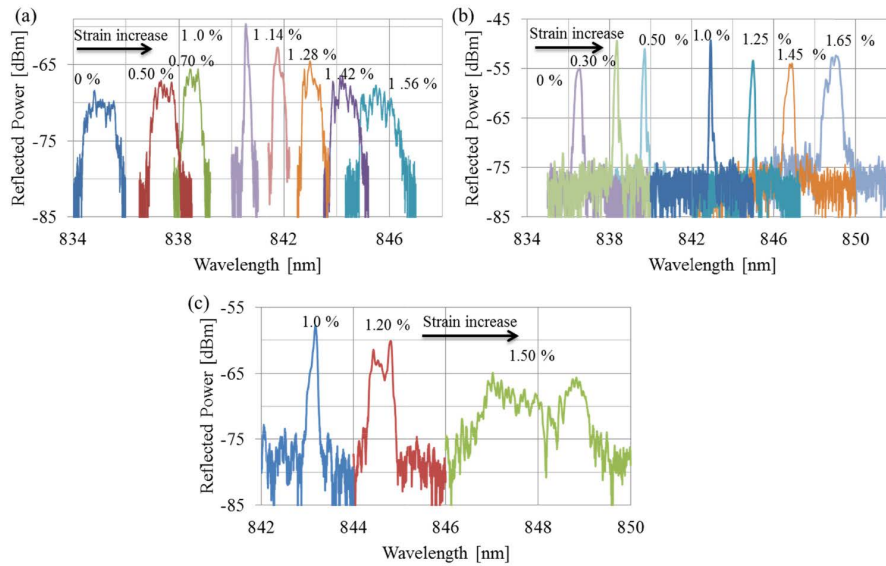


Fig. 5. Chirped FBG tunability by using strain on different tapers: (a) 9 μm/cm, (b) 4 μm/cm, (c) 14 μm/cm.

The recoverability of the grating with $r(0) = 63 \mu\text{m}$ and $r(L) = 59 \mu\text{m}$ has been examined through the strain increasing and decreasing processes. In the experiment, the strain was gradually applied to the grating up to 1.65% and then slowly decreased to zero strain. Judging from the variation of the resonance wavelengths and the peak intensities of the grating during the increasing-decreasing experiment, hysteresis is observed in the resonance wavelength and intensity as displayed in Fig. 6. Figures 6(a) shows a maximum variation of 4.7 dB of the peak intensities during the increasing-decreasing experiments, observed at a strain of 0.75%. Figures 7(b) shows the maximum resonance wavelength change, around 0.5 nm, which is achieved at a strain of 0.3%. Also, Fig. 6(b) shows the chirped POFBG response as a function of the strain and an average sensitivity of $0.71 \pm 0.02 \text{ pm}/\mu\epsilon$ is achieved. The reflected bandwidth vs strain is shown in Fig. 6(c), and indicates a great potential to explore when large strain is applied to the chirped POFBG.

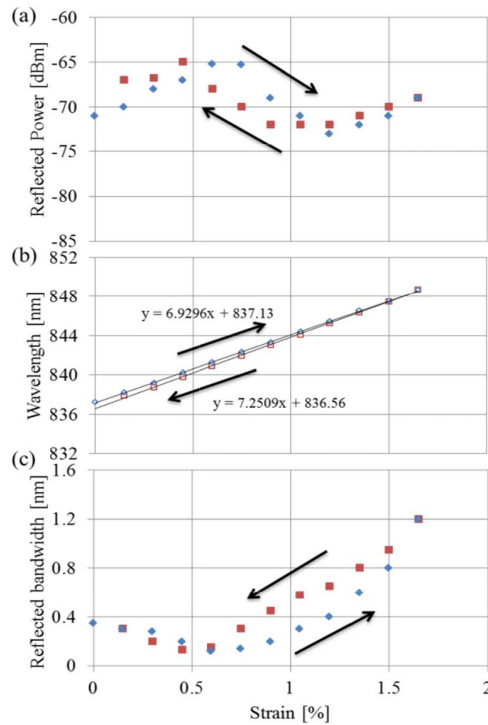


Fig. 6. Strain increasing-decreasing cycle of chirped POFBG (Fiber 1): (a) reflected peak power, (b) resonance wavelength and (c) reflected bandwidth.

A tapered section of Fiber 2 [20] with $r(0) = 66.5 \mu\text{m}$ and $r(L) = 61 \mu\text{m}$ was irradiated to produce chirped POFBGs with the same conditions presented in previous cases. The results under different strains are shown in Fig. 7(a) and indicate that etching technology for chirped POFBGs fabrication can be explored using POFs with different characteristics such as fiber diameter. From Fig. 7(a) we can also achieve a high sensitivity level. The bandwidths of three different tapered samples (with both fiber types) are shown in Fig. 7(b), indicating that stronger tapers lead to broader bandwidths.

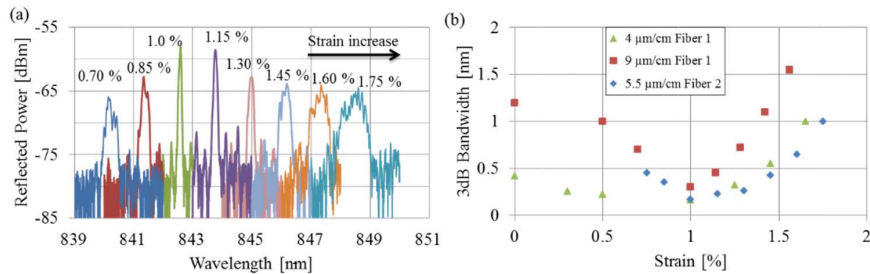


Fig. 7. (a) Reflected power spectrum of a $5.5 \mu\text{m}/\text{cm}$ tapered chirped Bragg grating under different strain using Fiber 2, (b) 3dB bandwidth of POFBG using three different tapered samples vs strain.

A chirped POFBG based on Fiber 1 was placed in the climatic chamber (Angelantoni Industrie CH340) with 50% humidity under varying temperature values. The temperature was

increased from 22 °C to 52 °C with steps of 5 °C and each temperature value was held during 10 minutes. Figure 8(a) shows the chirped POFBG response as a function of the temperature and a sensitivity of $-56.7 \text{ pm}/^\circ\text{C}$ is achieved (see Fig. 8(b)). Regarding to reflected bandwidth response, it keeps close to stable as shown in Fig. 8(c).

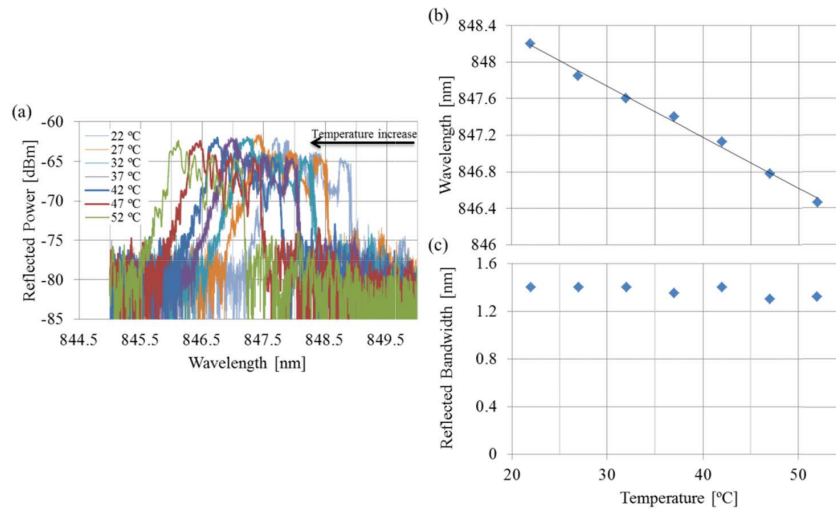


Fig. 8. (a) Dependence of the reflected power spectrum of chirped FBG under 1.6% strain on the temperature, (b) Central wavelength vs temperature under 1.6% strain, (c) Reflected 3 dB bandwidth vs temperature under 1.6% strain.

Figure 9(a) shows the grating stability under two-hours monitoring in the second day after fabrication. The grating shows a stable response with less than 1.5 dB decrease in reflected power. Also Fig. 9(b) shows the same grating one week later and the measurement confirms the stability of the spectral profile and strength although higher level of noise was measured due to significant connectorization losses. A shift of 0.5 nm is observed which can be attributed to random changes in environmental conditions, such as temperature and air humidity variations, being responsible for the observed drift of the Bragg peaks positions within $\pm 0.5 \text{ nm}$ margin.

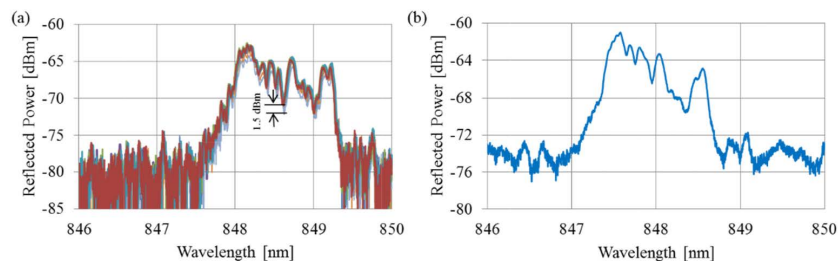


Fig. 9. (a) Grating stability in two hours monitoring under 1.6% strain, (b) response after one week under 1.6% strain.

5. Conclusion

We demonstrated the fabrication of tunable chirped Bragg gratings in polymer optical fiber using a uniform phase mask for the first time to our knowledge. Chirped POFBGs fabricated with different tapered profiles indicate the potentiality of this method. The strain and temperature sensitivity measurements demonstrate their tunability properties. By proper etching of the section we obtained 2.6 nm reflected bandwidth under 1.50% strain, and stronger tapered profiles would lead to chirped POFBGs with broader bandwidths. This work paves the way for different photonics applications of chirped fiber Bragg grating in POF.

Funding

Fundação para a Ciência e Tecnologia (FCT)/MEC (UID/EEA/50008/2013, SFRH/BPD/109458/201); Research Excellence Award Programme GVA (PROMETEO 2017/103); Fundamental Research Funds for the Heilongjiang Provincial Universities (KJCXZD201703).

Acknowledgments

This work was supported by Fundação para a Ciência e Tecnologia (FCT)/MEC through national funds and when applicable co-funded by FEDER – PT2020 partnership agreement under the project UID/EEA/50008/2013. C. A. F. Marques also acknowledges the financial support from FCT through the fellowship SFRH/BPD/109458/2015. The authors also acknowledge the Research Excellence Award Programme GVA PROMETEO 2017/103 FUTURE MICROWAVE PHOTONIC TECHNOLOGIES AND APPLICATIONS and Fundamental Research Funds for the Heilongjiang Provincial Universities (KJCXZD201703). We are grateful to Prof. Ole Bang and Dr. David Sáez-Rodríguez for providing the polymer optical fiber used in this work.